Article:
Wang, Y, Yu, Q, Mishra, B et al. (2018) Adsorption of Methylmercury onto Geobacter bemidijensis Bem. Environmental Science and Technology, 52 (20). pp. 11564-11572. ISSN: 0013-936X

https://doi.org/10.1021/acs.est.8b01987

Adsorption of methylmercury onto *Geobacter bemidijensis* Bem

Yuwei Wang[a], Qiang Yu[b], Bhoopesh Mishra[c], Jeffra K. Schaefer[a], Jeremy B. Fein[b], and Nathan Yee[a,*]

[a]Department of Environmental Sciences, Rutgers University, New Brunswick, New Jersey 08901, United States

[b]Department of Civil & Environmental Engineering & Earth Sciences, University of Notre Dame, Notre Dame, Indiana 46556, United States

[c]School of Chemical and Process Engineering, University of Leeds, Leeds LS2 9JT, United Kingdom

*Corresponding author: nyee@envsci.rutgers.edu

Submitted to *Environmental Science & Technology*

Abstract

The anaerobic bacterium *Geobacter bemidijensis* Bem has the unique ability to both produce and degrade methylmercury (MeHg). While the adsorption of MeHg onto bacterial surfaces can affect the release of MeHg into aquatic environments as well as the uptake of MeHg for demethylation, the binding of MeHg to the bacterial envelope remains poorly understood. In this study, we quantified the adsorption of MeHg onto *G. bemidijensis* and applied X-ray absorption spectroscopy (XAS) to elucidate the mechanism of MeHg binding. The results showed MeHg adsorption onto *G. bemidijensis* cell surfaces was rapid and occurred via complexation to thiol functional groups. Titration experiments yielded cell surface thiol concentrations of 3.2 to 6.4 μmol/g (wet cells). A one-site adsorption model with MeHg binding onto thiol sites provided excellent fits to adsorption isotherms conducted at different cell densities. The log K binding constant of MeHg onto the thiol sites was determined to be 10.2 ± 0.2. These findings provide a quantitative framework to describe MeHg binding onto bacterial cell surfaces and elucidate the importance of bacterial cells as possible carriers of adsorbed MeHg in natural aquatic systems.

Introduction

Anaerobic bacteria play a central role in the production and degradation of methylmercury (MeHg) in the environment.[1-3] In anoxic systems, net MeHg accumulation has been shown to be controlled by the balance of Hg methylation and MeHg demethylation rates,[4, 5] which are strongly influenced by microbe-mercury interactions. Adsorption of MeHg onto bacterial cells is an important process that occurs during both mercury methylation and demethylation.[6-10] MeHg adsorption onto Hg-methylating bacteria can affect the release of MeHg into aquatic environments,[8] while MeHg adsorption onto methylmercury degrading bacteria may limit the uptake of MeHg for enzymatic demethylation processes.[9-13] Currently, the adsorption affinity and binding mechanism of MeHg onto bacterial cells are poorly understood.

Previous studies have found that thiol functional groups on bacterial surfaces are reactive moieties involved in heavy metal binding.[14-20] Despite the low abundance of thiol sites relative to the total metal binding sites in bacterial membranes, metals such as Cd(II) preferentially bind to thiol functional groups under low metal loading conditions.[19] At environmentally relevant metal:biomass ratios, thiol sites also dominate the adsorption of Zn(II) and Ni(II).[17] Recently, Yu and Fein (2017)[20] showed that the adsorption of Hg(II), Cd(II), and Au(III) onto the Gram positive bacterium *Bacillus subtilis* is strongly enhanced by the elevated concentration of thiol sites within the cell envelopes. To date, the role of thiol functional groups in the adsorption of MeHg onto bacterial surface has not been characterized.

Geobacter bemidijensis Bem is a subsurface bacterium[21, 22] that has been reported to both produce and degrade methylmercury.[10, 23] This gram-negative anaerobe carries the mercury methylation genes *hgcAB*,[10, 24] which enables *G. bemidjiensis* to convert inorganic Hg(II) to MeHg. Additionally, in contrast to other *Geobacter* species, strain Bem also carries a homolog of

the alkylmercury lyase gene *merB*,[10] which confers the ability to demethylate MeHg. Both of these mercury methylation and demethylation pathways are intracellular reactions that require transport across the cell envelope to occur. In the case of mercury methylation, MeHg produced by the bacterium can bind onto cell surface ligands thus influencing the release of MeHg into the dissolved phase. For methylmercury degradation, adsorption of MeHg onto the cell envelop can affect MeHg uptake and transport into the cell. A quantitative understanding of MeHg adsorption on cell surface functional groups would thus improve our ability to model Hg transformations by *G. bemidijensis* and the distribution of MeHg during methylation and demethylation.

In this study, we conducted bulk adsorption experiments and spectroscopic analyses to investigate MeHg adsorption onto *G. bemidijensis* Bem. The objectives of this study were to (1) quantify the extent of MeHg adsorption onto *G. bemidijensis* cells; (2) characterize the local coordination environment of methylmercury adsorbed onto *G. bemidijensis* cells; and (3) develop a surface complexation model to describe the MeHg adsorption reaction. The results of this study provide new insights into the mechanism of MeHg adsorption onto an environmentally-relevant Hg methylating and MeHg-degrading bacterium.

Materials and Methods

Bacterial Culture and Assay Conditions: Strain *Geobacter bemidjiensis* Bem (gifted from B. Gu, Oakridge National Lab) was cultured at 30 °C under a nitrogen (N_2) headspace in ATCC Medium 1957 containing 40 mM fumarate and 30 mM acetate at pH 6.8. Cells were harvested at late exponential phase in an anaerobic glovebox, centrifuged for 8 min at 7900 g, and washed three times in 0.5 mM deoxygenated hypotonic MOPS buffer adjusted to 7.0 ± 0.2

with NaOH. Cells were then re-suspended in the MOPS buffer to a desired cell density for the MeHg adsorption experiments.

Methylmercury Adsorption Experiments: A methylmercury chloride stock solution (50 μM) was prepared by diluting a standard solution (1000 ppm; Alfa Aesar) with deoxygenated Ultrapure Water (18.2 MΩ cm^{-1}) and stored in an ultrahigh-purity N_2 atmosphere. The MeHg stock solution was analyzed for both total mercury (THg) and MeHg, and the purity was determined to be >99% MeHg before experimentation. Inside a glove box (Coy; 5:95 H_2:N_2 headspace), MeHg adsorption experiments were initiated by adding known amounts of MeHg to each foil-wrapped serum bottles containing 100 mL *G. bemidjiensis* washed cells suspension, capped with a Teflon-lined butyl rubber stopper and sealed with aluminum caps. The reactors were then shaken at 60 rpm at 30 °C. To examine the adsorption kinetics, individual reactors were sacrificed at specific time points for mercury analyses. Aliquots were taken for THg, total methylmercury (TMeHg), cell associated Hg ($MeHg_{cell}$), aqueous Hg ($MeHg_{aq}$), and intracellular Hg ($MeHg_{in}$) measurements. $MeHg_{cell}$ samples were collected by filtering the cell suspensions through 0.2 μm Isopore™ polycarbonate membrane filters. $MeHg_{aq}$ was determined by analyzing the filtrate of samples filtered through 0.2 μm PVDF syringe filters. $MeHg_{in}$ was determined by removing the adsorbed MeHg using a wash protocol modified from Schaefer et al. (2009).[25] Briefly, the adsorbed MeHg was removed by rinsing filtered cell suspensions with 5 mL of an oxalic acid-EDTA-Cl buffer twice and then with 5 mL 100 mM cysteine for 5 min. The concentration of adsorbed Hg ($MeHg_{ads}$) was calculated as the difference between $MeHg_{cell}$ and $MeHg_{in}$. Finally, TMeHg measurements were performed and compared with THg values to verify that methylmercury degradation did not occur during the experiment.

To determine MeHg binding constants, adsorption isotherm experiments were performed by adding 10-500 nM MeHg to individual batch reactors containing cell densities ranging from 3 g/L to 0.03 g/L (wet wt). After 2 h of equilibration, samples were collected from each reactor and digested for THg, $MeHg_{cell}$, and $MeHg_{aq}$ analyses. MeHg adsorption experiments at 3 g/L cells were repeated using *G. bemidjiensis* cells treated with 200 μM of Thiol Fluorescent Probe IV (TFP-4) (EMD Millipore Corporation) to block cellular thiol sites.[26, 27] Cells were treated with TFP-4 in a glove box and shaken in the dark for 2 h then washed three times with MOPS buffer before the adsorption experiment. Adsorption isotherms were modeled using FITEQL 2.0[28] to determine the apparent equilibrium constant of MeHg binding onto *G. bemidjiensis* and TFP-4 treated cells. R^2 values were calculated to determine the goodness of fit.

Mercury Analysis: TMeHg samples were preserved in 0.1 M H_2SO_4 at 4 °C, distilled by a Tekran 2750 gas manifold and heating system (EPA method 1630) and analyzed using Tekran 2700 gas chromatography coupled to cold vapor atomic fluorescence spectroscopy (GC−CVAFS). All other samples were digested in bromine monochloride to a final concentration of 0.02 M at 60 °C for at least 48 h and then analyzed by either cold vapor atomic fluorescence spectrometry using a Brooks Rand MERX Total Mercury Analytical System (EPA Method 1631) or cold vapor atomic absorption using a Leeman Laboratories Hydra AA Mercury Analyzer (EPA Method 245.1).

Determination of Thiol Functional Groups on Cell Surface: The abundance of thiol functional groups on the cell surface of *G. bemidjiensis* was quantified by the fluorescence-based method of Joe-Wong et al. (2012) using qBBr (monobromo(trimethylammonio)bimane bromide) (Sigma-Aldrich).[29] QBBr is a positively charged compound that forms highly fluorescent thioether bonds with exposed thiol moieties on the cell surface whose fluorescence increases

prominently upon conjugation.[30] The positive charge of the molecule makes it difficult to pass through the inner membrane, thus allowing qBBr to preferential react with cell envelope thiol sites. In the titration experiment, qBBr was added at specific concentrations (0-35 μM) to *G. bemidjiensis* cell suspensions (3 g/L) and then allowed to react in the dark for 2 h in a 30°C shaker. The fluorescence was then measured in 1-mL quartz cuvettes at an excitation wavelength of 400 nm and peak emission intensity of 465 nm with a Molecular Devices Plate Reader.

In addition to the fluorescence approach, potentiometric titrations of *G. bemidjiensis* cell suspensions were also performed to quantify the total surface site concentration.[31] This acid-base titration method measures the concentration of proton-active sites within bacterial cell envelopes. The difference in the proton-active site concentration before and after the thiols are blocked using a qBBr treatment was used to determine the concentration of thiol sites within the cell envelope. Cells were treated with ~1 mM qBBr for 2 h in the dark and washed three times with 0.1 M NaCl to remove excess qBBr before the titration experiments. Titrations were conducted using an autotitrator assembly with 10 g/L *G. bemidjiensis* or qBBr-treated cells suspended in 0.1 M NaCl. Aliquots of 1 M HCl were added to the cell suspensions to adjust the pH to 3.0, followed by titration with 1 M NaOH to raise the pH to 9.7. These base titrations were the portion of the dataset used in the titration modeling. Three titrations experiments were conducted for *G. bemidjiensis*, and then triplicate experiments were repeated for qBBr-treated cells. All of the titrations were performed under a N_2 gas headspace to exclude atmospheric CO_2. The titration data were modeled using FITEQL 2.0 to determine the thiol concentration and acid dissociation constant (pKa) of the proton-active surface functional groups. The number of surface sites was systematically varied in the model to determine the number of discrete sites

155 required to fit the experimental data. The goodness of fit of each tested model was evaluated by
156 comparing the values of the residual function, V(Y), from the FITEQL 2.0 output.

157 **X-ray Absorption Spectroscopy**: *G. bemidjiensis* cells with adsorbed MeHg were
158 analyzed using X-ray absorption spectroscopy. Cell suspensions (3 g/L) were reacted with 50 nM
159 or 500 nM MeHg for 2 h, pelleted by centrifugation, and freeze dried. After grinding the freeze
160 dried cells to a fine powder in an anaerobic chamber, the samples were placed in Teflon sample
161 holders, covered with Kapton thin film, and sealed with Kapton tape. The samples were then
162 placed in deoxygenated containers in slotted flexiglass sample holder sandwiched between
163 Kapton tape separated by thin Kapton film and shipped to the Advanced Photon Source at
164 Argonne National Laboratory for XAS analysis. Hg LIII-edge EXAFS spectra were collected at
165 beamline 13-ID-E, GeoSoilEnviroCARS, using a Si (111) monochromatic crystal with a 13-
166 element germanium detector. Samples were run under a N_2 atmosphere at ambient temperature
167 and pressure. Energy calibration was performed such that the first inflection points of Au foil and
168 HgSn amalgam were assigned as 11 919 and 12 284 eV, respectively. The beam was focused to
169 200 μm × 200 μm. Quick scans (5 min/scan) were performed on MeHg samples collecting 3
170 scans each at over 20 separate spots for each sample to limit the beam-induced chemistry and get
171 highly reproducible scans. Data were processed using ATHENA and ARTEMIS.[32] The k-space
172 data range used for these analyses are 2.5 to 8.0 $Å^{-1}$, using a Hanning window function dk set to
173 1.0. $S0^2$ of 0.9 was used with during simultaneous fitting of 68 μg /g and 455 μg /g MeHg-cell
174 samples at multiple (1, 2, and 3) k weighting. Statistically significant lower reduced chi-square
175 was used for inclusion of another atom in shell by shell fitting approach. R-factor of 1.5% was
176 obtained for a fit range of 1.1 to 3.0 Å in Fourier transformed R space.

177

Results and Discussion

MeHg adsorption onto *G. bemidijensis* Bem cell surfaces. Kinetics experiments showed that *G. bemidijensis* rapidly sorbed MeHg, with approximately 80% of MeHg sorbing in 15 minutes (Fig. 1A). MeHg sorption was concurrent to the removal of MeHg from solution. To determine the intracellular versus surface-bound distribution of cell-associated MeHg, a 100 mM cysteine solution was used to desorb MeHg on the cell surface. Approximately 95-100% of the sorbed MeHg was extracted by reaction with cysteine (Fig.1B), indicating that almost all the MeHg was surface-bound and less than 5% of the MeHg was internalized. Adsorption isotherms were then conducted at different cell densities to determine the affinity of MeHg adsorption onto *G. bemidijensis* (Fig. 2). The data showed that the concentration of adsorbed MeHg increased linearly with the aqueous MeHg concentration (Fig 2A-C). To test if thiol sites are involved in MeHg adsorption, a thiol-specific probe TFP-4 was used to block the thiol sites associated with the bacterial cells. The TFP-4 treated cells adsorbed markedly less MeHg (Fig. 2D) compared to untreated cells (Fig. 2A). The decrease in MeHg adsorption was attributed to the loss of thiol complexation in the TFP-4 treated cells.

Quantification of thiol sites. Two independent types of experiments were conducted to determine the concentration of thiol sites on cell surface of *G. bemidijensis*. First, we conducted a titration experiment using the fluorescent probe qBBr which binds specifically to sulfhydryl sites within the cell envelope. When reacted with the qBBr fluorophore, the fluorescence emission increased steeply and linearly with increasing qBBr concentration until the cell surface thiol sites became saturated with qBBr (Fig. 3A). Further additions of qBBr showed weak fluorescence emission with increasing qBBr concentration, as this excess qBBr remained unbound to thiol sites and hence did not strongly fluoresce. The best-fit lines of the two linear

regions of the qBBr titration curve showed an inflection point at 3.2 μmol/g wet cells, corresponding to the concentration of reactive thiols on the cell surface of *G. bemidijensis*.

In the second experiment, we conducted acid-base potentiometric titrations with *G. bemidijensis* washed cell suspensions to quantify the concentration of proton-active sites on the cell surface (Fig 3B). Replicate titrations yielded an average total site concentration of 253.0 ± 2.9 μmol/g (wet weight). The titration curves were modeled using FITEQL 2.0 to determine individual site concentrations according the reaction:

$$R\text{-}L_iH \rightleftharpoons R\text{-}L_i^- + H^+ \quad (1)$$

where $[R\text{-}L_iH]$ and $[R\text{-}L_i^-]$ represent the concentrations of the *i*th neutral and deprotonated organic acid functional group on the bacterial cell surface, respectively. The acidity constant of each surface site type was quantified with the corresponding mass action equation:

$$K_{a,i} = \frac{\left[R\text{-}L_i^-\right] a_{H^+}}{[R\text{-}L_iH]} \quad (2)$$

A four site model provided the best-fit to the titration data. The best-fit model yielded pKa values of 3.9 ± 0.4, 5.4 ± 0.3, 7.2 ± 0.2, and 9.6 ± 0.1 with corresponding site concentrations of 76.0 ± 7.6, 70.3 ± 11.1, 37.9 ± 4.0 and 68.8 ± 5.1 μmol/g, respectively (Table 1). We repeated the titrations with cells that were treated with qBBr to block the thiol sites on the cell surface, and the resulting titration curves were fit with a four site model. The model yielded very similar pKa values to those from the titrations using the untreated cells (Table 1). A decrease of approximately 6.4 μmol/g was observed in the site concentration for site 4 when cell surface thiols were blocked by qBBr. A previous study also showed significant changes in concentration of site 4 (pKa 9.2–9.4) of bacterial strains *Bacillus licheniformis*, *Bacillus subtilis*, *Bacillus*

222 *cereus*, *Shewanella oneidensis* and *Pseudomonas fluorescens* when thiols were blocked by
223 qBBr.[31] Furthermore, the pKa value of site 4 is similar to that of thiol molecules such as cysteine,
224 glutathione and some proteins, with values ranging from 8.06 to 10.75.[33] Therefore, we suggest
225 that site 4 likely represents a mixture of site types, some of which are thiol functional groups,
226 and all of which exhibiting similar pKa values. Together with the qBBr fluorescence titration
227 experiment (Fig. 3A), we estimate the concentration of cell surface thiols to be between 3.2 and
228 6.4 μmol/g.

229 **XAS Analysis of Adsorbed MeHg.** X-ray absorption spectroscopy was performed to
230 examine the local binding environment of the adsorbed MeHg. The first derivative of normalized
231 X-ray absorption near edge structure (XANES) and the X-ray absorption fine structure (XAFS)
232 spectra of *G. bemidijensis* reacted with 50 nM and 500 nM MeHg are displayed in Figure 4A and
233 B, respectively. The amount of MeHg adsorbed to those two samples were 68 μg /g and 455 μg
234 /g, respectively. Derivative of the XANES spectra of the two samples were nearly identical and
235 both spectra exhibited two main peaks (Fig 4A). The energy difference between the two peaks
236 was used to calculate the ΔE value. Because a larger ΔE corresponds to Hg-ligand complexes
237 with ionic character and a smaller ΔE to complexes with more covalent character,[34] we used this
238 value to infer the local bonding environment of MeHg. The derivative of the XANES spectra
239 showed a ΔE value of 7.0 eV, which is similar to ΔE values of Hg-cysteine$_2$ (ΔE = 7.2 eV)[35, 36]
240 and MeHg-cysteine (ΔE = 7.7 eV).[37] K^2 weighted χ(k) spectra of the 68 μg /g and 455 μg /g
241 samples were nearly identical and no phase shift in the k^2 weighted χ(k) XAFS oscillations
242 between the two samples was observed (Fig. 4B). This indicates that the stoichiometry of MeHg-
243 cell complexes was the same at the two different MeHg loadings. Both 68 μg /g and 455 μg /g
244 samples were best fit with 0.9 +/- 0.1 sulfur atom at ~2.34 angstrom and 0.9 +/ 0.1 carbon atom

245 at ~2.03 angstrom, indicating that the Hg-C bond in MeHg remained intact when adsorbed on the
246 bacterial surface and that MeHg was bonded exclusively to thiol sites of *G. bemidjiensis* (Fig 4C
247 and 4D, Table 4). No changes in the Hg–S bond distance was observed suggesting that the
248 MeHg–S complexes were the same in both samples (Fig 4C and 4D). Notably, the binding
249 distance and the ratios of Hg atoms to C and S atoms are similar to MeHg-DOM bonding.[38-43]

250 **MeHg Adsorption Constant.** Because the XAFS data showed MeHg binding to the thiol
251 functional groups with a 1:1 MeHg:site stoichiometry (Fig 4B, Table 3), the adsorption
252 isotherms were used to determine a stability constant for the MeHg-thiol complex formed on the
253 cell surface using the following reaction:

254 $$R\text{-}L_4^- + MeHg^+ \rightleftharpoons R\text{-}L_4\text{-}MeHg \quad (3)$$

255 where R-L_4-MeHg is the MeHg adsorbed onto the cell surface, and R-L_4^- is the thiol portion of
256 site 4 with a pKa value of 9.5 and a thiol concentration of 6.4 μmol/g as determined by the acid-
257 base titration experiments. The stability constant was quantified with the corresponding mass
258 action equation:

259 $$K_{MeHg\text{-}L4} = \frac{[R\text{-}L_4\text{-}MeHg]}{[R\text{-}L_4^-]\, a_{MeHg^+}} \quad (4)$$

260 The MeHg binding constant was remarkably consistent for three adsorption data sets. At cell
261 concentration of 3 g/L, 0.6 g/L and 0.3 g/L, the adsorption data yielded log $K_{MeHg\text{-}L4}$ values of
262 10.1 ± 0, 10.3 ± 0.1, and 10.2 ± 0.1, respectively (Table 2). The model fits displayed in Figure 2
263 show good agreement with the experimental data. The one-site model for MeHg binding onto R-
264 L_4^- provided excellent fits to all three adsorption isotherms with r^2 values greater than 0.95
265 (Table 2). No improvement in fit was obtained using a two-site model by including an additional

site for MeHg binding. Combining all data sets, the average log K value for the one site model was 10.2 ± 0.2. This binding constant is comparable to log K values of MeHg complexation to aquatic humic and fulvic acids which range from 10.7 to 14.8 for binding reactions with the same stoichiometry as is shown in Reaction 3. [38, 44-46]

We then modeled the adsorption isotherm of the thiol-blocked cells (Fig. 2D). First, we tested a one-site adsorption model with MeHg binding to site 1. The resulting log K value for MeHg binding was 3.8 with a corresponding r^2 value of 0.96. Because our data were not collected as a function of pH, the binding site for MeHg is not well-constrained. Therefore, we also considered MeHg binding to alternate cell surface sites (e.g., sites 2, 3 or 4). The resulting calculated binding constant was the highest for site 4 with a log K value of 6.4 (Table 2). None of the models with the alternate sites improved the goodness of fit. Including an additional site for adsorption using a two-site model also did not improve the goodness of fit. Because site 1 has the lowest pKa value and the highest site density, the concentration of deprotonated sites at the pH conditions of the adsorption experiments for site 1 is greater than the other sites. Thus, we tentatively assign site 1 as the binding site for MeHg onto the thiol-blocked cells. We note that the stability constant for this R-L_1-MeHg complex (log K = 3.8) is significantly lower than the R-L_4-MeHg complex (log K = 10.2), thereby offering an explanation as to why MeHg binds exclusively to thiol sites as observed in the EXAFS experiments. Although site 1 is much more abundant than the thiols in site 4, the relative K values indicate that the thiol sites exhibit an affinity to bind MeHg that is orders of magnitude greater than that exhibited by site 1. Since MeHg binding to site 1 is much weaker than MeHg complexation to the thiol sites, we propose that site 1 likely corresponds to a weak organic acid ligand such as a carboxyl functional group.

Environmental Implications

The rapid and extensive adsorption of MeHg onto *G. bemidijensis* indicates that cell surfaces are reactive interfaces that can accumulate MeHg produced by Hg-methylating bacteria. The adsorption model presented in this study provides a quantitative framework to understand MeHg binding to the cell envelope of *Geobacter* species during MeHg production. Previous studies have shown that approximately 80% of the MeHg produced by *G. bemidijensis* is adsorbed onto cell surfaces[10] and more than 90% of MeHg is bound to *G. sulfurreducens* PCA.[8] The amount of adsorbed MeHg measured in these previous experiments is in agreement with the distribution of MeHg predicted by our surface complexation model. Because MeHg binds strongly to cell surfaces during methylation, the fate of this adsorbed MeHg is expected to be tied to that of the bacterial cells. For example, if the Hg-methylating bacteria are mobile, then the adsorbed MeHg would be carried along with the particulate phase for environmental transport. MeHg is known to be partitioned onto particulate matter in aquatic environments,[47, 48] where bacterial cells typically represent a significant fraction of the particulate phase. [49, 50] Conversely, if the bacterial cells are attached to sediment surfaces or form biofilms, then the adsorbed MeHg would have limited environmental mobility.

Our results suggest that the concentration of cellular thiols is an important factor that controls the extent to which bacterial cells can act as carriers of adsorbed MeHg. The concentration of thiols on bacterial surfaces appears to vary between bacterial species. Whereas *G. bemidijensis* has at most 6.4 μmol/g of cell surface thiol sites, the closely related Hg-methylating bacterium *G. sulfurreducens* PCA has at least 10 times higher reactive thiols in its cell envelope.[16] In comparison, the non Hg-methylating bacteria *B. cereus*, *B. subtilis* and *S. oneidensis* have intermediate cell surface thiol concentrations of 16.6, 22.5, and 33.1 μmol/g.[31]

312 Notably, these values are in the same order of magnitude as thiol concentrations found in solid
313 organic particles (~22 μmol/g),[51] and hence bacteria are likely to be able to compete effectively
314 with solid organic particles for available MeHg in aquatic systems.

315 The desorption of MeHg from the *G. bemidijensis* is facilitated by aqueous complexation
316 with strong ligands such as cysteine (Fig. 1B). Likewise, in natural systems the release of MeHg
317 from bacterial surfaces would be enhanced by the presence of low-molecular-weight thiol
318 compounds or other high affinity aqueous ligands. This can occur through interactions with
319 certain humic and fulvic acids which have been shown to complex MeHg with binding constants
320 of log $K > 14$.[38, 44, 46] Natural waters containing high concentrations of dissolved thiols and
321 aqueous sulfide[52] would also favor the desorption process. Interestingly, MeHg desorption from
322 Hg-methylation bacteria may stimulate additional methylation to occur. Lin et al. (2015)[8] found
323 that the amount of MeHg produced by *G. sulfurreducens* PCA increases when cysteine is added
324 to desorb cell-bound MeHg. Thus, adsorption-desorption reactions may play an important but
325 poorly understood role in affecting net methylmercury production by *Geobacter* species. The
326 stability constants determined in this study will improve quantitative models to describe the
327 competition of environmentally-relevant ligands in MeHg binding and for estimating the fate and
328 distribution of MeHg in the environment.

329 MeHg adsorbed to marine particles containing bacterial cells have been shown to
330 demethylate MeHg,[48] suggesting an interplay between adsorption and MeHg degradation. In
331 experiments with *G. bemidijensis* Bem, Lu et al. (2016)[10] observed that the concentration of
332 adsorbed MeHg decreases during MeHg degradation. It is currently unknown if adsorbed MeHg
333 is bioavailable and directly internalized for demethylation. Recently, Ndu et al. (2016)[12]
334 demonstrated that non-specific binding of MeHg to cellular ligands decreases the rates of MeHg

degradation, thus suggesting that adsorbed MeHg is unavailable for direct uptake. In this case, adsorbed MeHg must first desorb into the aqueous phase and then re-enter the cell via passive or active transport for demethylation. Identification of the cell surface molecules that harbor the high affinity MeHg binding sites and elucidation of the MeHg uptake pathway in *G. bemidijensis* are needed to better understand the role of adsorption in the MeHg demethylation process.

354 **Acknowledgements**

355 This research was supported by the U.S. National Science Foundation grants EAR-1760534 and
356 EAR-1424950. GeoSoilEnviroCARS is supported by the U.S. National Science Foundation
357 (EAR-0622171) and Department of Energy - Geosciences (DE-FG02-94ER14466). Use of the
358 Advanced Photon Source was supported by the U. S. Department of Energy, Office of Science,
359 Office of Basic Energy Sciences, under Contract No. DE-AC02-06CH11357. We thank Tony
360 Lanzirotti and Matt Newville for technical support and insights.

References

(1) Compeau, G.; Bartha, R., Sulfate-reducing bacteria: principal methylators of mercury in anoxic estuarine sediment. *Appl. Environ. Microbiol.* **1985,** *50*, (2), 498-502.

(2) Pak, K.-R.; Bartha, R., Mercury methylation and demethylation in anoxic lake sediments and by strictly anaerobic bacteria. *Appl. Environ. Microbiol.* **1998,** *64*, (3), 1013-1017.

(3) Marvin-DiPasquale, M.; Agee, J.; McGowan, C.; Oremland, R. S.; Thomas, M.; Krabbenhoft, D.; Gilmour, C. C., Methyl-mercury degradation pathways: a comparison among three mercury-impacted ecosystems. *Environ. Sci. Technol.* **2000,** *34*, (23), 4908-4916.

(4) Avramescu, M.-L.; Yumvihoze, E.; Hintelmann, H.; Ridal, J.; Fortin, D.; Lean, D. R., Biogeochemical factors influencing net mercury methylation in contaminated freshwater sediments from the St. Lawrence River in Cornwall, Ontario, Canada. *Sci. Total Environ* **2011,** *409*, (5), 968-978.

(5) Tjerngren, I.; Karlsson, T.; Björn, E.; Skyllberg, U., Potential Hg methylation and MeHg demethylation rates related to the nutrient status of different boreal wetlands. *Biogeochemistry* **2012,** *108*, (1-3), 335-350.

(6) Gilmour, C. C.; Elias, D. A.; Kucken, A. M.; Brown, S. D.; Palumbo, A. V.; Schadt, C. W.; Wall, J. D., Sulfate-reducing bacterium *Desulfovibrio desulfuricans* ND132 as a model for understanding bacterial mercury methylation. *Appl. Environ. Microbiol.* **2011,** *77*, (12), 3938-3951.

(7) Graham, A. M.; Bullock, A. L.; Maizel, A. C.; Elias, D. A.; Gilmour, C. C., Detailed assessment of the kinetics of Hg-cell association, Hg methylation, and methylmercury degradation in several *Desulfovibrio* species. *Appl. Environ. Microbiol.* **2012,** *78*, (20), 7337-7346.

(8) Lin, H.; Lu, X.; Liang, L.; Gu, B., Thiol-Facilitated Cell Export and Desorption of Methylmercury by Anaerobic Bacteria. *Environ. Sci. Technol.lett.* **2015,** *2*, (10), 292-296.

(9) Lu, X.; Gu, W.; Zhao, L.; Haque, M. F. U.; DiSpirito, A. A.; Semrau, J. D.; Gu, B., Methylmercury uptake and degradation by methanotrophs. *Sci. Adv.* **2017,** *3*, (5), e1700041.

(10) Lu, X.; Liu, Y.; Johs, A.; Zhao, L.; Wang, T.; Yang, Z.; Lin, H.; Elias, D. A.; Pierce, E. M.; Liang, L.; Barkay, T.; Gu, B., Anaerobic Mercury Methylation and Demethylation by *Geobacter bemidjiensis* Bem. *Environ Sci Technol* **2016,** *50*, (8), 4366-73.

(11) Barkay, T.; Miller, S. M.; Summers, A. O., Bacterial mercury resistance from atoms to ecosystems. *FEMS Microbiol Rev* **2003,** *27*, (2-3), 355-384.

(12) Ndu, U.; Barkay, T.; Schartup, A. T.; Mason, R. P.; Reinfelder, J. R., The effect of aqueous speciation and cellular ligand binding on the biotransformation and bioavailability of methylmercury in mercury-resistant bacteria. *Biodegradation* **2016,** *27*, (1), 29-36.

(13) Silva, P. J.; Rodrigues, V., Mechanistic pathways of mercury removal from the organomercurial lyase active site. *PeerJ.* **2015,** *3*, e1127.

(14) Mishra, B.; Boyanov, M.; Bunker, B. A.; Kelly, S. D.; Kemner, K. M.; Fein, J. B., High-and low-affinity binding sites for Cd on the bacterial cell walls of *Bacillus subtilis* and *Shewanella oneidensis*. *Geochim. Cosmochim. Acta* **2010,** *74*, (15), 4219-4233.

(15) Mishra, B.; O'Loughlin, E. J.; Boyanov, M. I.; Kemner, K. M., Binding of HgII to high-affinity sites on bacteria inhibits reduction to Hg(0) by Mixed FeII/III phases. *Environ. Sci. Technol.* **2011,** *45*, (22), 9597-9603.

(16) Mishra, B.; Shoenfelt, E.; Yu, Q.; Yee, N.; Fein, J. B.; Myneni, S. C., Stoichiometry of mercury-thiol complexes on bacterial cell envelopes. *Chem. Geol.* **2017,** *464*, 137-146.

(17) Nell, R. M.; Fein, J. B., Influence of sulfhydryl sites on metal binding by bacteria. *Geochim. Cosmochim. Acta* **2017,** *199*, 210-221.

(18) Wang, Y.; Schaefer, J. K.; Mishra, B.; Yee, N., Intracellular Hg (0) oxidation in *Desulfovibrio desulfuricans* ND132. *Environ. Sci. Technol.* **2016,** *50*, (20), 11049-11056.

(19) Yu, Q.; Fein, J. B., The effect of metal loading on Cd adsorption onto *Shewanella oneidensis* bacterial cell envelopes: the role of sulfhydryl sites. *Geochim. Cosmochim. Acta* **2015,** *167*, 1-10.

(20) Yu, Q.; Fein, J. B., Enhanced removal of dissolved Hg (II), Cd (II), and Au (III) from water by *Bacillus subtilis* bacterial biomass containing an elevated concentration of sulfhydryl sites. *Environ. Sci. Technol.* **2017,** *51*, (24), 14360-14367.

(21) Nevin, K. P.; Holmes, D. E.; Woodard, T. L.; Hinlein, E. S.; Ostendorf, D. W.; Lovley, D. R., *Geobacter bemidjiensis* sp. nov. and *Geobacter psychrophilus* sp. nov., two novel Fe(III)-reducing subsurface isolates. *Int J Syst Evol Microbiol* **2005,** *55*, (Pt 4), 1667-74.

(22) Holmes, D. E.; O'neil, R. A.; Vrionis, H. A.; N'guessan, L. A.; Ortiz-Bernad, I.; Larrahondo, M. J.; Adams, L. A.; Ward, J. A.; Nicoll, J. S.; Nevin, K. P., Subsurface clade of *Geobacteraceae* that predominates in a diversity of Fe (III)-reducing subsurface environments. *ISME J* **2007,** *1*, (8), 663-677.

(23) Gilmour, C. C.; Podar, M.; Bullock, A. L.; Graham, A. M.; Brown, S. D.; Somenahally, A. C.; Johs, A.; Hurt Jr, R. A.; Bailey, K. L.; Elias, D. A., Mercury methylation by novel microorganisms from new environments. *Environ. Sci. Technol.* **2013,** *47*, (20), 11810-11820.

(24) Parks, J. M.; Johs, A.; Podar, M.; Bridou, R.; Hurt, R. A.; Smith, S. D.; Tomanicek, S. J.; Qian, Y.; Brown, S. D.; Brandt, C. C., The genetic basis for bacterial mercury methylation. *Science* **2013,** *339*, (6125), 1332-1335.

(25) Schaefer, J. K.; Morel, F. M., High methylation rates of mercury bound to cysteine by *Geobacter sulfurreducens*. *Nat. Geosci.* **2009,** *2*, (2), 123.

(26) Campuzano, I. D.; San Miguel, T.; Rowe, T.; Onea, D.; Cee, V. J.; Arvedson, T.; McCarter, J. D., High-throughput mass spectrometric analysis of covalent protein-inhibitor adducts for the discovery of irreversible inhibitors: a complete workflow. *J Biomol Screen* **2016,** *21*, (2), 136-144.

(27) Yi, L.; Li, H.; Sun, L.; Liu, L.; Zhang, C.; Xi, Z., A highly sensitive fluorescence probe for fast thiol-quantification assay of glutathione reductase. *Angew. Chem. Int. Ed* **2009,** *48*, (22), 4034-4037.

(28) Westall, J. C., *FITEQL: A computer program for determination of chemical equilibrium constants from experimental data.* Department of Chemistry Oregon State University: 1982.

(29) Joe-Wong, C.; Shoenfelt, E.; Hauser, E. J.; Crompton, N.; Myneni, S. C., Estimation of reactive thiol concentrations in dissolved organic matter and bacterial cell membranes in aquatic systems. *Environ. Sci. Technol.* **2012,** *46*, (18), 9854-9861.

(30) Kosower, N. S.; Kosower, E. M.; Newton, G. L.; Ranney, H. M., Bimane fluorescent labels: labeling of normal human red cells under physiological conditions. *Proc. Natl. Acad. Sci. U.S.A.* **1979,** *76*, (7), 3382-3386.

(31) Yu, Q.; Szymanowski, J.; Myneni, S. C.; Fein, J. B., Characterization of sulfhydryl sites within bacterial cell envelopes using selective site-blocking and potentiometric titrations. *Chem. Geol.* **2014,** *373*, 50-58.

(32) Ravel, B.; Newville, M., ATHENA and ARTEMIS: interactive graphical data analysis using IFEFFIT. *Phys. Scr.* **2005,** *2005*, (T115), 1007.

(33) Tajc, S. G.; Tolbert, B. S.; Basavappa, R.; Miller, B. L., Direct determination of thiol pK a by isothermal titration microcalorimetry. *J. Am. Chem. So* **2004,** *126*, (34), 10508-10509.

(34) Powers, L., X-ray absorption spectroscopy application to biological molecules. *Biochim. Biophys. Acta, Rev.* **1982,** *683*, (1), 1-38.

(35) Colombo, M. J.; Ha, J.; Reinfelder, J. R.; Barkay, T.; Yee, N., Anaerobic oxidation of Hg (0) and methylmercury formation by *Desulfovibrio desulfuricans* ND132. *Geochim. Cosmochim. Acta* **2013,** *112*, 166-177.

(36) Colombo, M. J.; Ha, J.; Reinfelder, J. R.; Barkay, T.; Yee, N., Oxidation of Hg (0) to Hg (II) by diverse anaerobic bacteria. *Chem. Geol.* **2014,** *363*, 334-340.

(37) Rajan, M.; Darrow, J.; Hua, M.; Barnett, B.; Mendoza, M.; Greenfield, B. K.; Andrews, J. C., Hg L3 XANES study of mercury methylation in shredded Eichhornia crassipes. *Environ. Sci. Technol.* **2008,** *42*, (15), 5568-5573.

(38) Hintelmann, H.; Welbourn, P. M.; Evans, R. D., Measurement of complexation of methylmercury (II) compounds by freshwater humic substances using equilibrium dialysis. *Environ. Sci. Technol.* **1997,** *31*, (2), 489-495.

(39) Karlsson, T.; Skyllberg, U., Bonding of ppb levels of methyl mercury to reduced sulfur groups in soil organic matter. *Environ. Sci. Technol.* **2003,** *37*, (21), 4912-4918.

(40) Qian, J.; Skyllberg, U.; Frech, W.; Bleam, W. F.; Bloom, P. R.; Petit, P. E., Bonding of methyl mercury to reduced sulfur groups in soil and stream organic matter as determined by X-ray absorption spectroscopy and binding affinity studies. *Geochim. Cosmochim. Acta* **2002,** *66*, (22), 3873-3885.

(41) Ravichandran, M., Interactions between mercury and dissolved organic matter--a review. *Chemosphere* **2004,** *55*, (3), 319-31.

(42) Skyllberg, U.; Qian, J.; Frech, W., Combined XANES and EXAFS study on the bonding of methyl mercury to thiol groups in soil and aquatic organic matter. *Phys. Scr.* **2005,** *2005*, (T115), 894.

(43) Yoon, S.-J.; Diener, L. M.; Bloom, P. R.; Nater, E. A.; Bleam, W. F., X-ray absorption studies of CH_3Hg^+-binding sites in humic substances. *Geochim. Cosmochim. Acta* **2005,** *69*, (5), 1111-1121.

(44) Amirbahman, A.; Reid, A. L.; Haines, T. A.; Kahl, J. S.; Arnold, C., Association of methylmercury with dissolved humic acids. *Environ. Sci. Technol* **2002,** *36*, (4), 690-695.

(45) Hintelmann, H.; Welbourn, P.; Evans, R., Binding of methylmercury compounds by humic and fulvic acids. *Water Air Soil Pollut* **1995,** *80*, (1-4), 1031-1034.

(46) Khwaja, A. R.; Bloom, P. R.; Brezonik, P. L., Binding strength of methylmercury to aquatic NOM. *Environ. Sci. Technol* **2010,** *44*, (16), 6151-6156.

(47) Cardona-Marek, T.; Schaefer, J.; Ellickson, K.; Barkay, T.; Reinfelder, J. R., Mercury speciation, reactivity, and bioavailability in a highly contaminated estuary, Berry's Creek, New Jersey Meadowlands. *Environ. Sci. Technol* **2007,** *41*, (24), 8268-8274.

(48) Ortiz, V. L.; Mason, R. P.; Ward, J. E., An examination of the factors influencing mercury and methylmercury particulate distributions, methylation and demethylation rates in laboratory-generated marine snow. *Mar chem* **2015,** *177*, 753-762.

(49) Weiss, P.; Schweitzer, B.; Amann, R.; Simon, M., Identification in situ and dynamics of bacteria on limnetic organic aggregates (lake snow). *Appl. Environ. Microbiol.* **1996,** *62*, (6), 1998-2005.

(50) Böckelmann, U.; Manz, W.; Neu, T. R.; Szewzyk, U., Characterization of the microbial community of lotic organic aggregates ('river snow') in the Elbe River of Germany by cultivation and molecular methods. *FEMS Microbiol Ecol* **2000,** *33*, (2), 157-170.

(51) Skyllberg, U.; Drott, A., Competition between disordered iron sulfide and natural organic matter associated thiols for mercury (II)- An EXAFS study. *Environ. Sci. Technol.* **2010,** *44*, (4), 1254-1259.

(52) Dyrssen, D.; Haraldsson, C.; Westerlund, S.; Årén, K., Indication of thiols in Black Sea deep water. *Mar. Chem.* **1985,** *17*, (4), 323-327.

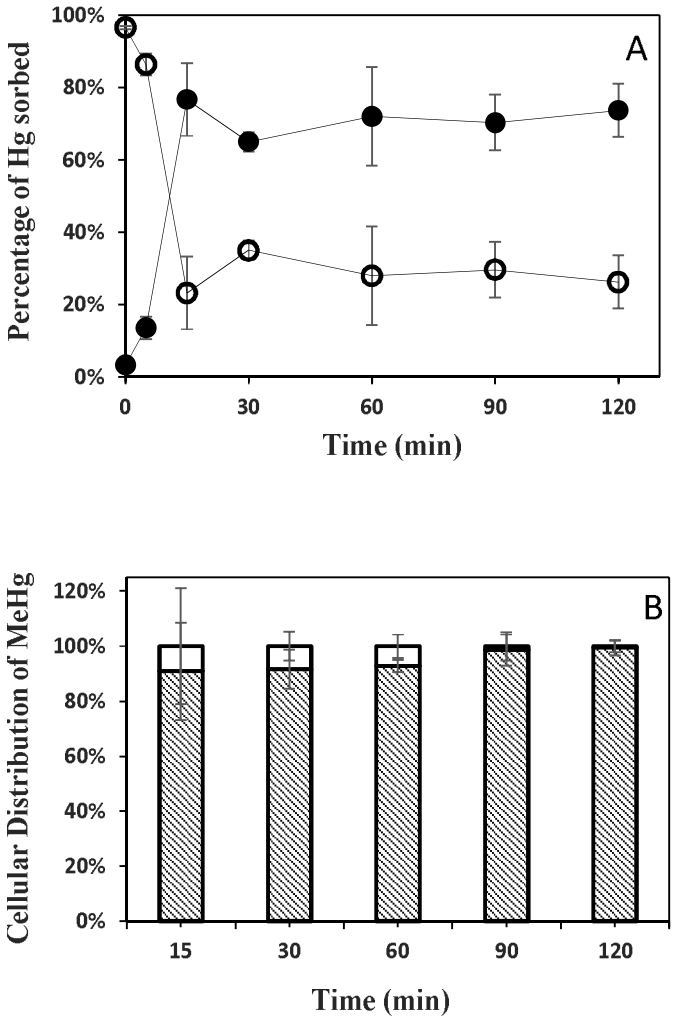

Figure 1. MeHg adsorption onto *Geobacter bemidjiensis* Bem. (A) MeHg adsorbed on *G. bemidjiensis* Bem (closed circles) and the aqueous concentration of MeHg remaining in solution (open circles); (B) Intracellular MeHg (solid white) and cell surface adsorbed MeHg (shaded pattern). Experiments were conducted in MOPS buffer with cell density of 3 g/L (wet wt) and a total MeHg concentration of 50 nM. Error bars represent 1σ values of triplicate experiments.

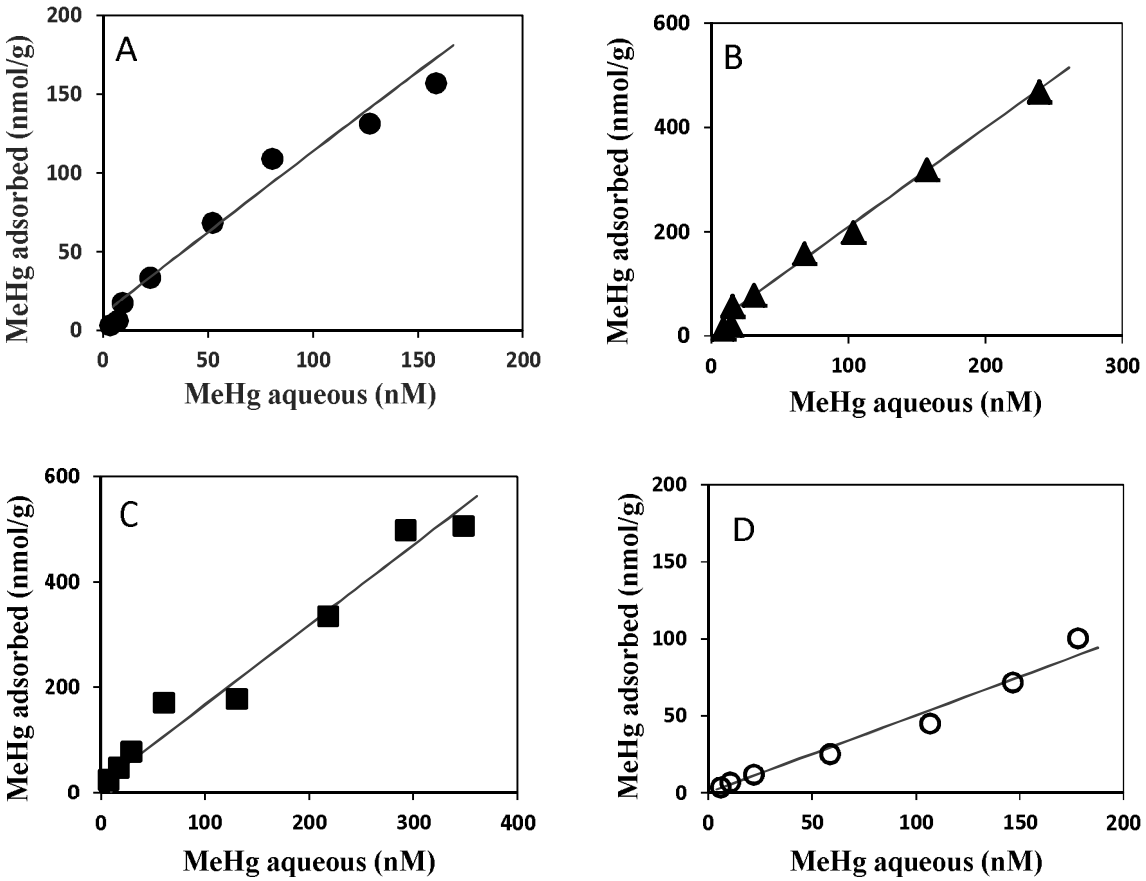

Figure 2. MeHg adsorption isotherms conducted at different cell densities: (A) 3 g/L, (B) 0.6 g/L, (C) 0.3 g/L. (D) MeHg adsorption isotherm conducted with TFP-4 treated cells (3 g/L). The solid black lines represent the best fitting one-site adsorption model.

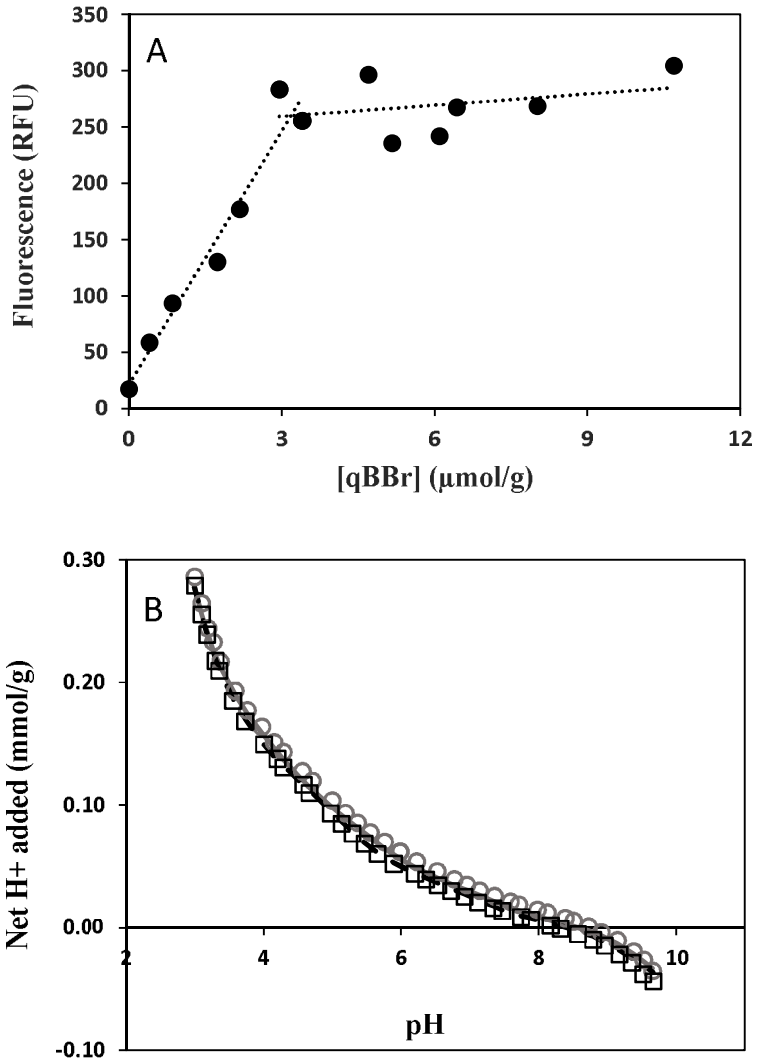

Figure 3. Quantification of reactive thiols on the cell surface of *G. bemidjiensis*. (A) Fluorescence intensities of *G. bemidjiensis* reacted with varying qBBr concentrations. Experiments were conducted at a cell density of 3 g/L and each data point represents an individual experiment. (B) Representative acid-base titration curves of *G. bemidjiensis* cells (open circles) and thiol-blocked cells (open squares). The best-fitting 4-site nonelectrostatic surface complexation model for *G. bemidjiensis* and thiol-blocked cells are depicted by the solid and dashed curves, respectively.

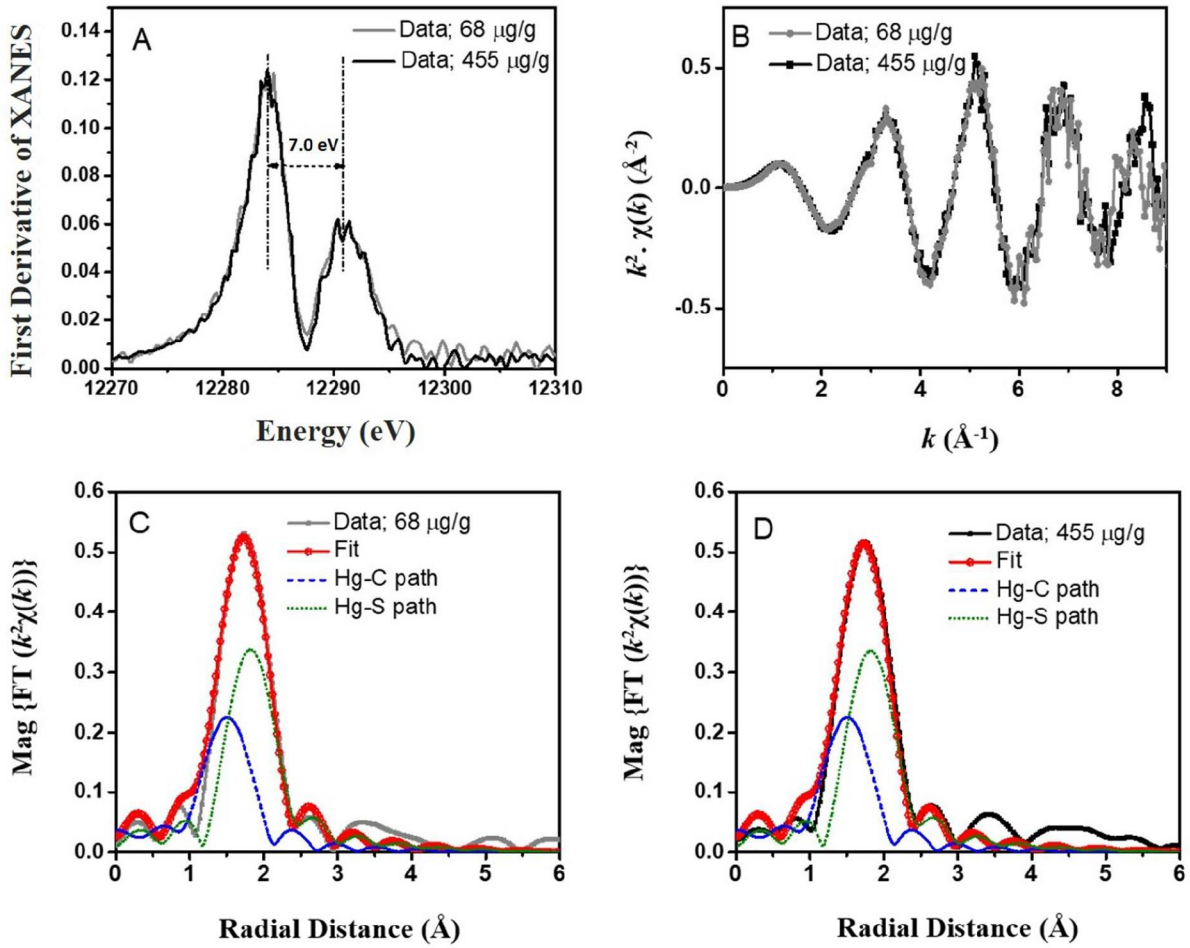

Figure 4. Structure characterization and fit of MeHg-reacted *G. bemidjiensis* by X-ray absorption spectroscopy analysis. (A) Derivative of normalized XANES; (B) The k^2-weighted EXAFS data of 68 μg/g and 455 μg/g MeHg adsorbed bacterial samples; (C) Magnitude of EXAFS Fourier-transformed data and along with Hg-C and Hg-S signal contributions for 68 μg/g samples; and (D) Magnitude of EXAFS Fourier-transformed data and along with Hg-C and Hg-S signal contributions for 455 μg/g sample.

Table 1. Surface site concentrations and acidity constants of *G. bemidjiensis* with and without qBBr treatment

	pKa_1	Sites 1 (µmol/g)	pKa_2	Site 2 (µmol/g)	pKa_3	Site 3 (µmol/g)	pKa_4	Site 4 (µmol/g)
Untreated	3.9 ± 0.4	76.0 ± 7.6	5.4 ± 0.3	70.3 ± 11.1	7.2 ± 0.2	37.9 ± 4.0	9.6 ± 0.1	68.8 ± 5.1
qBBr-Treated	3.8 ± 0.2	73.3 ± 7.5	5.2 ± 0.1	77.4 ± 5.3	7.1 ± 0.1	38.6 ± 1.0	9.5 ± 0.1	62.4 ± 8.4

Table 2. Log K values for MeHg adsorption onto *G. bemidjiensis* Bem and thiol-blocked cells.

	Cell density[a]	Surface site	Log K[b]	R^2
Geobacter bemidijensis	3 g/L	Site 4	10.1 ± 0.2	0.95
	0.6 g/L	Site 4	10.3 ± 0.1	0.98
	0.3 g/L	Site 4	10.2 ± 0.1	0.96
Thiol-blocked *Geobacter bemidijensis*	3 g/L	Site 1	3.8 ± 0.1	0.96
	3 g/L	Site 2	3.8 ± 0.1	0.96
	3 g/L	Site 3	4.5 ± 0.1	0.96
	3 g/L	Site 4	6.4 ± 0.1	0.96

[a]wet weight.
[b]Log K adsorption constants with corresponding 1σ uncertainty.

Table 3. XAFS best fit values for simultaneous modeling of MeHg adsorbed onto *G. bemidjiensis*

	Path	N	R (Å)	$\sigma^2 \times 10^{-3}$ (Å^2)	ΔE (eV)	S_0^2
68 µg/g MeHg	Hg-C	0.9 ± 0.1	2.03 ± 0.01	3.3 ± 2.1	1.2 ± 1.4	0.9
	Hg-S	0.9 ± 0.1	2.34 ± 0.01	1.8 ± 1.1		
455 µg/g MeHg	Hg-C	0.9 ± 0.1	2.03 ± 0.01	3.3	1.2 ± 1.4	0.9
	Hg-S	0.9 ± 0.1	2.34 ± 0.01	1.8		